

Attosecond light pulses to reveal the time-dependent rovibrational motion of the correlated electron pair in helium

Toru Morishita¹, Shinichi Watanabe¹ and C. D. Lin²

¹*Department of Applied Physics and Chemistry, University of Electro-Communications,
1-5-1 Chofu-ga-oka, Chofu-shi, Tokyo 182-8585, Japan*

²*Department of Physics, Kansas State University, Manhattan, KS 66506, USA*

(Dated: May 24, 2019)

We illustrate how attosecond light pulses can be used to directly mapping out the time-dependence of the correlated motion of two excited atomic electrons, discuss how the two-electron correlations manifest themselves in realistic attosecond measurements, and propose the following for experimental exploration: (a) The single ionization signals which directly reveal bending-vibrational motion of the correlated electron pair, (b) and also its rotational motion. (c) The double ionization signals which directly reveal the two-electron density in momentum space. To facilitate the description of the above points, use is made of simple wave packets of doubly-excited states of helium.

PACS numbers: 32.80.Qk,32.80.Fb,31.25.Jf,31.15.Ja

Following the recent developments in intense laser physics, ultra-short XUV (extreme ultraviolet) light pulses with duration of several hundred attoseconds (or a few atomic units) have been reported[1, 2, 3]. Such pulse durations are comparable to the time scale of the electronic motion in the ground and the lower excited states of atoms and molecules, thus opening up the route to the time-resolved study of electron dynamics in matter, akin to the time-resolved tracking of the atomic motion in a molecule enabled by the advent of femtosecond laser pulses[4]. In terms of probing electron dynamics, the only time-domain measurement reported so far is the determination of Auger lifetime by Drescher *et al.*[2], although other applications of attosecond pulses have been reported elsewhere[5, 6]. Unlike molecules where the time-dependent rotational and vibrational motions have clear classical meaning, the significance of the time-dependence of the electronic motion is presently elusive. The root of this misapprehension lies in the shell model of atoms which currently forms the basis for interpretation of almost all the energy-domain measurements. According to this model, each electron is moving in an effective central-field potential made of the electron-nucleus interaction plus an average potential due to the remaining electrons. Thus the time dependence of the interaction of one electron with the others is often probed in the form of a relaxation, which tends to be monotonic. Standard atomic structure theory accounts for the deviations of the central field model in terms of configuration interaction (CI). Thus in the time-domain study of electron dynamics, the time-dependent CI coefficients are calculated[7]. The point is that such coefficients carry little physical meaning, and one must resort to some alternative viewpoint for a physical interpretation.

In this Letter we suggest that a good place to study the time-domain electron dynamics is where the breakdown of the shell model is most severe, namely to probe multiply excited states of an atom using attosecond XUV pulses. Theoretical studies in the past decades have revealed that the shell model fails completely for these

states[8, 9, 10, 11, 12, 13, 14, 15, 16], and the motions of electrons in these states are better described by drawing analogy with the rotation and vibration of a floppy polyatomic molecule, where the periods are of the order of a few to sub-femtoseconds. By using doubly excited states of helium as an example, we show that the rotational and bending vibrational motions of the two electrons can be probed directly with XUV attosecond pulses, where single and/or double ionization signals of coherently populated doubly excited states should reveal these rotational and/or vibrational motions directly. For these systems, the “movies” of the correlated motion of the two electrons can be made to reveal their time evolution, similar to the “movies” showing the motion of atoms in a molecule. However, there is a significant difference. The rotational and the vibrational periods in a molecule are at least two orders of magnitude different. Thus their motions are not directly coupled. For atoms, the rotational and vibrational periods are comparable. To disentangle the various rotational and bending vibrational modes would require a careful preparation of the initial coherent double excited states. Addressing the preparation of such coherent doubly excited states is not a purpose of this Letter. Instead, we consider simplest initial coherent states and calculate the time-dependence of the ionization yield to show that they indeed reveal the rotational and the bending motion of the two electrons directly.

To describe the collective motion of the two electrons in the doubly excited states[11], it is convenient to look at them as a linear XY_2 triatomic molecule, with X playing the role of the nucleus and Y an electron. Instead of the independent electron coordinates \mathbf{r}_1 and \mathbf{r}_2 , the wavefunctions are to be expressed in terms of R , $\Omega_v = (\alpha, \theta_{12})$ for the internal stretching and bending vibrational motions, and three Euler angles $\Omega_r = (\alpha', \beta', \gamma')$ for the overall rotational motions. Here the hyperradius R and the hyperangle α are defined by $r_1 = R \cos \alpha$ and $r_2 = R \sin \alpha$. Thus R stands for the size of the atom, α measures the relative distances of the two electrons from

the nucleus, and θ_{12} is the angle which the two electrons make with the nucleus at the vertex. Note that each wavefunction depends on six variables excluding spins. For visualization, the vibrational and rotational mode of each state can be defined via the densities,

$$\rho_j^{\text{vib}}(\alpha, \theta_{12}) = \int |\varphi_j|^2 d\Omega_r dR,$$

$$\rho_j^{\text{rot}}(\Omega_r) = \int |\varphi_j|^2 d\Omega_v dR$$

for each state φ_j . In presenting $\rho^{\text{rot}}(\Omega_r)$, we choose $\hat{\mathbf{r}}_1 - \hat{\mathbf{r}}_2$ and $\hat{\mathbf{r}}_1 \times \hat{\mathbf{r}}_2$ to be parallel to the z' - and y' -axes of the body-fixed frame, respectively. We consider linearly polarized laser pulses parallel to the z -axis of the space-fixed frame. Thus, we only need to consider the magnetic component of the total angular momentum, $M = 0$, so that the density does not depend on γ' .

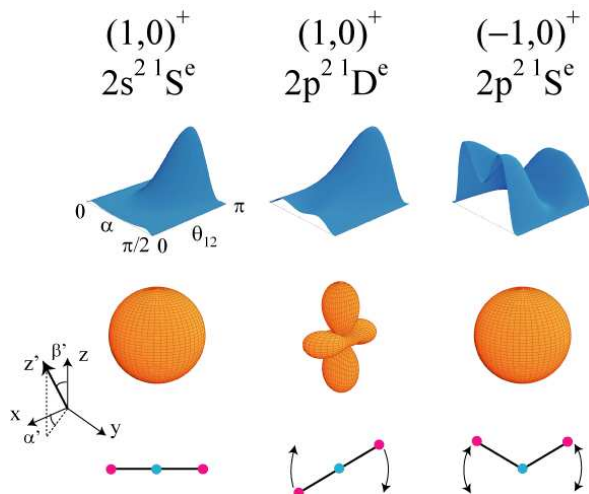


FIG. 1: (color online). Density plots of the doubly excited states. The top row presents the relief plots of $\rho^{\text{vib}}(\alpha, \theta_{12})$, and the middle row shows $\rho^{\text{rot}}(\alpha', \beta')$ by polar plots. As seen from the density plots, $2s^2 1S^e$, $2s^2 1D^e$, and $2p^2 1S^e$ are considered as ground, rotationally excited, and vibrationally excited states, respectively. The bottom row sketches the corresponding classical rotational and bending vibrational modes of the two correlated electrons.

Neglecting autoionization for the time being, consider first the “stationary” doubly excited states, conventionally called $2s^2 1S^e$, $2p^2 1S^e$, and $2p^2 1D^e$ states. These states exhibit large configuration mixing and are more accurately classified using the $(K, T)^A$ quantum numbers as described in [11]. In this designation, the three states are denoted as $(K, T)^A = (1, 0)^+$, $(-1, 0)^+$, and $(1, 0)^+$, respectively. In Fig. 1 the vibrational and rotational densities of each state are given, together with a classical sketch of the motion of the two electrons.

For $2s^2 1S^e$, $\rho^{\text{vib}}(\alpha, \theta_{12})$ has a maximum at $\theta_{12} = \pi$ and $\rho^{\text{rot}}(\Omega_v)$ is isotropic. Thus, this state is considered as the ground state of the ro-vibrational motion. For $2p^2 1D^e$, $\rho^{\text{vib}}(\alpha, \theta_{12})$ has maximum at $\theta_{12} = \pi$ similar to $2s^2 1S^e$, but $\rho^{\text{rot}}(\Omega_r)$ has nodes in β' similar to

$|Y_{20}(\beta', \alpha')|^2$ due to total angular momentum $L = 2$ with $T = 0$. That is, this state is rotationally excited. For $2p^2 1S^e$, on the contrary, ρ^{rot} is isotropic, but there is a nodal line in $\rho^{\text{vib}}(\alpha, \theta_{12})$ at about $\theta_{12} = \pi/2$, so that this state is an excited state in the bending-vibrational mode. With this understanding, we proceed to discuss how to observe the time-dependence of these rotational and vibrational motions by first creating coherent states by a pump pulse. We will then consider the use of attosecond light pulses for probing the time dependence of the coherent state via the ionization yield. To this end, we calculated the ionization probability from such coherent doubly excited states by applying the time-dependent Hyperspherical method[17] to the single ionization, and the first order perturbation theory to the double ionization separately.

We highlight the following three points in turn. (1) *Attosecond pulses probing bending vibrational motion.* When the $2s^2 1S^e$ and $2p^2 1S^e$ states are coherently excited at $t = 0$, a vibrational wave packet is created. We used a Gaussian attosecond pulse of mean energy of 21.8 eV, duration of 142 asec, and intensity of 3.5×10^{12} W/cm² to ionize this coherent state by stimulated emission. The resulting ionization yield of $\text{He}^+(1s)+e$ in the energy region of -2 to -1 a.u., as shown in the top frame of Fig. 2, shows the expected oscillations as a function of delay time. The oscillation has a period of about 970 asec, corresponding to the inverse of the energy separation between the two states, $2\pi/\Delta E$. In fact, this oscillation can be traced directly to the bending vibrational motion, as seen clearly from the calculated time evolution of the average angle between the two electrons with the nucleus at the vertex, $\langle \theta_{12} \rangle$. At the bottom of this figure, the calculated $\rho^{\text{vib}}(\alpha, \theta_{12})$ is shown over a period. The ionization probability peaks when the two electrons are mostly on opposite sides of the nucleus. We note that the ionization yield decreases with increasing delay time, due to the autoionization of the $2s^2 1S^e$ state which has a lifetime of about 5.4 fsec. Thus the ionization yield can be used to measure the lifetime of the shorter-lived state directly without the help of an IR laser[2]. Note that attosecond pulses are needed in order to see the identifiably rapid oscillations in the ionization probabilities.

(2) *Attosecond pulses probing the rotational motion.* In Fig. 3 we show the ionization probability of $\text{He}^+(1s)+e$ in the energy region of -2 to -1 a.u. vs delay time from a coherent state made of $2s^2 1S^e$ and $2p^2 1D^e$. In this case each state is the ground state of the vibrational motion. The time-dependent oscillation is to be traced to the rotational motion, since the $2p^2 1D^e$ state has total angular momentum $L = 2$ with $T = 0$, *i.e.*, it is rotationally excited in β' . The time dependence of the ionization probability is shown to follow the oscillation of the Euler angle β' . (The average of the deviation from $\pi/2$.) This angle β' is defined to be the angle between the “molecular axis” (the axis between the two electrons) with respect to the laser polarization direction. In this case, more ionization occurs when the line joining the two electrons

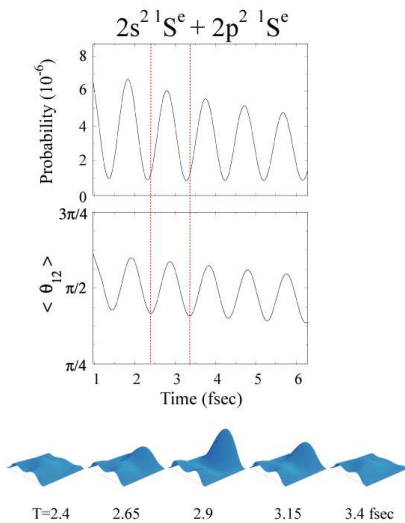


FIG. 2: (color online). Delay time dependence of (a) stimulated single ionization probability from a coherent doubly excited state of $[\varphi(2s^2^1S^e) + 2\varphi(2p^2^1S^e)]/\sqrt{5}$ of He, (b) the average angle between the two electrons with respect to the nucleus, and (c) the two electron density distributions over one period.

are parallel to the laser polarization. A more complete view of the rotational motion of the wave packet can be seen from the bottom frame where the rotational density evolution within one period is displayed. Note that the oscillation period (2.0 fsec) is inversely proportional to the energy separation between the two states.

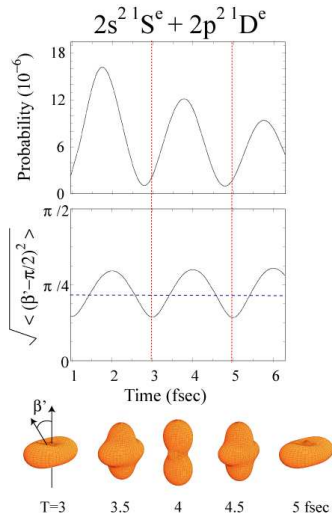


FIG. 3: (color online). Delay time dependence of (a) stimulated ionization probability from a coherent doubly excited state of $[\varphi(2s^2^1S^e) + \varphi(2p^2^1D^e)]/\sqrt{2}$ of He, (b) the average of the angle between the two-electron axis with respect to the laser polarization (see text), and (c) the rotational distributions of the atom in Euler angles.

(3) Attosecond pulses probing two-electron wavefunc-

tions in momentum space. The oscillation of the single ionization probabilities presented above is generic to any two-state system. The oscillation can be interpreted in terms of bending vibrational or rotational motions of the two electrons only when they are accompanied by such careful theoretical analysis as presented here. Without *a priori* information about the nature of the coherent state, a blind display of the six-dimensional two-electron wavefunction would not be able to reveal the nature of the two-electron dynamics. For an arbitrarily created coherent state, an ambiguous analysis of this sort would be rather difficult. We thus ask whether it is possible to map out the time-dependence of the two-electron motion directly. One method we propose is to measure double ionization of helium by an attosecond light pulse.

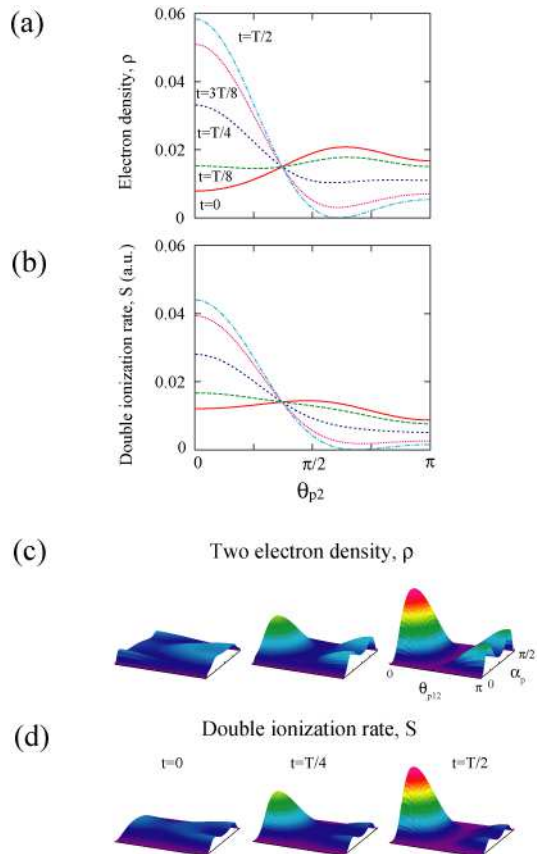


FIG. 4: (color online). Time-dependence of double ionization from a coherent state of $[\varphi(2s^2^1S^e) + \varphi(2p^2^1S^e)]/\sqrt{2}$. (a) The angular distribution of the electron density of the initial coherent state in momentum space. Shown is the momentum density of the second electron with respect to the direction of the fixed first electron; (b) The distribution of the calculated ionization signal of the second electron with respect to the direction of the fixed first electron; (c) The two-dimensional two-electron momentum space density distributions of the initial coherent state; (d) Double ionization signals showing the relative momentum distributions between the two ionized electrons. (see text).

We calculated the probability of double ionization by

an attosecond light pulse with mean energy of 27.2 eV and pulse duration of 83 asec. We use a weak light pulse so that double ionization probability is calculated by the first order perturbation theory. In the actual calculation, the velocity gauge was used and the electric field of the attosecond pulse was assumed Gaussian. The two free electrons in the final states are approximated by properly symmetrized products of plane waves. Under this approximation, one can formally show that in the limit of a very narrow pulse, the ionization probability is proportional to the two-electron charge density in the momentum space of the initial coherent state.

We have carried out a numerical calculation for the simplest coherent state made of $2s^2\ ^1S^e$ and $2p^2\ ^1S^e$. The double ionization probability $P(\mathbf{p}_1, \mathbf{p}_2, t)$ is a function of the six-dimensional momenta of the two electrons. Here t is the time that elapsed after the pump pulse. This particular example of a coherent state represents a bending vibrational wave packet. In Fig. 4(a) we plot the ionization rate $S(\mathbf{p}_1, \mathbf{p}_2, t) \propto P(\mathbf{p}_1, \mathbf{p}_2, t) / [\hat{\epsilon} \cdot (\mathbf{p}_1 + \mathbf{p}_2)]^2$ as a function of θ_{p2} , with fixed ejected electron energies of two electrons $e_1 = e_2 = 2.2$ eV and $\theta_{p1} = 0$, over half a period at $t = 0, T/8, T/4, 3T/8$, and $T/2$ asec (the total double ionization probability is expected to oscillate with a period of $T = 970$ asec for this coherent state) Here, the angles are measured relative to the laser polarization $\hat{\epsilon}$. In the upper frame, the density plots constructed from the momentum space wavefunction are shown. It is clear that the angular dependence of the ionization signal resembles the angular dependence of the momentum space electron density; see Fig. 4(b). Note that the amplitude of the oscillations in the ionization signal is somewhat weaker. This is due to the averaging effect from the finite pulse duration of 83 asec. (The mean energy of 27.2 eV was used, since such short attosecond pulses have to be generated from the plateau region of the high-order harmonics.)

We define the momentum space hyperspherical coordinates for the two electrons which enable us to similarly

define the momentum space counterpart of the vibrational and rotational densities. In Fig. 4(c) and (d) we compare the ionization measurement with the momentum space densities as functions of $\alpha_p = \arctan(p_2/p_1)$ and $\theta_{p12} = \arccos(\hat{\mathbf{p}}_1 \cdot \hat{\mathbf{p}}_2)$ [18, 19]. (Note that these angles are not conjugate to the hyperspherical coordinates variables in the configuration space, α and θ_{12} .) Indeed, the ionization signal clearly reproduces the bending vibrational density of the two electrons in the momentum space. Representing the final state wavefunctions by plane waves as in the present example is undoubtedly an over-simplification. Improved calculations might show slight distortions to the double ionization signals, a task left for future exploration. Nevertheless, it is undeniable that the present calculation points out that attosecond pulses are capable of mapping out the two-electron dynamics. Such information cannot be directly derived from energy-domain measurements.

In summary, we have shown that attosecond light pulses can be used to probe the correlated motion of two excited electrons. For properly created coherent states the rotational and/or bending vibrational modes of the two excited electrons can be directly mapped by the single or double ionization signals vs the time delay. Extension of the present analysis to multiply excited states[13, 16] and many-body systems would similarly offer a new perspective that distinguishes itself from the established energy-domain measurements.

This work was supported in part by a Grant-in-Aid for Scientific Research (C) from the Ministry of Education, Culture, Sports, Science and Technology, Japan, and by the 21st Century COE program on ‘‘Coherent Optical Science’’. This work was also supported by Chemical Sciences, Geosciences and Biosciences Division, Office of Basic Energy Sciences, Office of Science, U.S. Department of Energy. TM was also supported by financial aids from the Matsuo Foundation and the University of Electro-Communications. TM thanks Prof. H. Kono, Dr. X. M. Tong and Dr. Z. X. Zhao for useful discussions.

-
- [1] M. Hentschel *et al.*, Nature (London) **414**, 509 (2001).
 - [2] M. Drescher *et al.*, Nature (London) **419**, 803 (2002).
 - [3] T. Sekikawa, *et al.* Nature (London) **432**, 605 (2004).
 - [4] A. H. Zewail, J. Phys. Chem. **104**, 5660 (2000).
 - [5] E. Gouliemakis *et al.*, Science **305**, 1267 (2004).
 - [6] F. Lindner *et al.*, Phys. Rev. Lett. **95**, 040401 (2005).
 - [7] C. E. Nicolaides, *et al.*, Phys. B**35**, L271 (2002)
 - [8] J. W. Cooper, U. Fano, and F. Prats, Phys. Rev. Lett. **10**, 518 (1963).
 - [9] D. R. Herrick and O. Sinanoğlu, Phys. Rev. **11**, 97 (1975); M. E. Kellman and D. R. Herrick, J. Phys. B **11**, L755 (1978); O. Sinanoğlu and D. R. Herrick, J. Chem. Phys. **62**, 886 (1975); M. E. Kellman and D. R. Herrick, Phys. Rev. A **22**, 1536 (1980).
 - [10] G. S. Ezra and R. S. Berry, Phys. Rev. A **28**, 1974 (1983).
 - [11] C. D. Lin, Adv. At. Mol. Phys. **22**, 27 (1986).
 - [12] S. Watanabe and C. D. Lin, Phys. Rev. A **34**, 823 (1986).
 - [13] T. Morishita and C. D. Lin, Phys. Rev. A **67**, 022511 (2003).
 - [14] L. B. Madsen, J. Phys. B **36**, R223 (2003).
 - [15] M. D. Poulsen and L. B. Madsen, Phys. Rev. A **71**, 062502 (2005).
 - [16] T. Morishita and C. D. Lin, Phys. Rev. A **71**, 012504 (2005).
 - [17] T. Morishita, K. Hino, T. Edamura, D. Kato, S. Watanabe and M. Matsuzawa J. Phys. B: At. Mol. Opt. Phys. **34**, L475 (2001).
 - [18] D. Kato and S. Watanabe, Phys. Rev. A **56**, 003687 (1997).
 - [19] R. Peterkop, Theory of Ionization of Atom by Electron Impact (Colorado Associated University Press, Boulder, 1977).